
ZONAL DETACHED EDDY SIMULATION COUPLED WITH STEADY RANS IN THE WALL REGION

L. Davidson

Division of Fluid Dynamics, Department of Mechanics and Maritime Sciences
Chalmers University of Technology
SE-412 96 Gothenburg, Sweden
lada@chalmers.se

Abstract

Xiao *et al.* [1] proposed an interesting hybrid LES/RANS method in which they use two solvers and solve the RANS and LES equations in the entire computational domain. In the present work this method is simplified and used as a hybrid RANS-LES method, a *wall-modeled* DES. The two solvers are employed in the entire domain. Near the walls, the flow is governed by the steady RANS solver; drift terms are added to the LES equations to ensure that the time-filtered LES fields agree with the steady RANS field. Away from the walls, the flow is governed by the LES solver; the RANS field is set to the time-filtered LES field. The advantage of solving the steady RANS equations is that advanced RANS turbulence models can be used since these models were developed for steady RANS. The EARSM model is used in the RANS region. The new method is called **S-ZDES**.

1. Introduction

DES (Detached-Eddy Simulation) uses unsteady RANS near walls (URANS region) and LES further away from walls (LES region). The resolved turbulence in the URANS region is often larger than the modeled part. But the RANS models used in the URANS region were originally developed and tuned in steady RANS simulations. Hence the accuracy and the validity of the RANS models in the URANS region can be questioned. In the present work DES is coupled with *steady* RANS near the walls. We denote the method S-ZDES (steady RANS coupled to zonal DES).

Xiao *et al.* [1] proposed a new method in which they solve both the LES and RANS equations in the entire domain. The flow is in the near-wall region governed by the RANS equations and in the outer region it is governed by the LES equations. This is achieved by adding drift terms in the LES and RANS equations. In the interface region(s), the drift terms are modified by a linear ramp function. Drift terms are used in all equations in the RANS equations (momentum equations, the pressure equation (PISO is used)) and in the modelled turbulent equations (k and ϵ). Two drift terms are added in the LES momentum equations; one to ensure that the mean velocity field in the RANS and LES equations is the same and one to ensure that the total turbulent kinetic energies are the same.

In [2] they extended the method to account for non-conformal meshes. They used a Cartesian mesh for the LES equations and a body-fitted mesh for the RANS equations. They applied the method to fully developed channel flow and the flow over periodic hills. The paper shows how an accurate academic solver – massively parallel – can be combined with industrial, flexible RANS solvers.

Tunstall *et al.* [3] implement and use the method and modify it (different ramp function, different constants, reducing the number of case-specific constants etc). They apply it to fully developed channel flow and a rather complex flow consisting of a pipe junction including heat transfer. Hence, they have to introduce drift terms also in the energy equations.

Breuer and Schmidt [4] used an advanced RANS turbulence model – the Explicit Algebraic Reynolds Stress Model, EARSM – in a hybrid LES-RANS methodology. However, as mentioned above, the

disadvantage is that the RANS equations are solved in transient mode, where a large part of the large-scale turbulence is resolved.

In the present study, the steady RANS equations are solved. Here it makes sense to use advanced RANS turbulence models, since these models were developed for steady RANS. The EARSM [5] is used in the RANS solver. The present method is in many aspects similar to that proposed in [1, 3] but it is simplified: the RANS equations are used in steady mode, a more advanced RANS turbulence model is used and the present method includes fewer drift terms and tuning constants.

2. The S-ZDES methodology

The domain is split into a steady RANS region (S-RANS) and LES region (LES), see Fig. 1. Two sets of equations (steady RANS, see Fig. 1a and unsteady DES, see Fig. 1b) are solved in the entire domain on identical grids although the steady RANS mesh may be two dimensional (as in the present work). Drift terms are added in the LES equations, S_i^{LES} , in the S-RANS region. The drift terms in the LES velocity equations read

$$S_i^{LES} = \frac{v_i^{RANS} - \langle \bar{v}_i^{LES} \rangle_T}{\Delta t} \quad (1)$$

No drift term is used in the pressure equation. $\langle \cdot \rangle$ indicates integration over time, T , i.e.

$$\langle \phi(t) \rangle_T = \frac{1}{T} \int_{-\infty}^t \phi(\tau) \exp(-(t-\tau)/T) d\tau \Rightarrow \langle \phi \rangle_T^{n+1} \equiv \langle \phi \rangle_T = a \langle \phi \rangle_T^n + (1-a) \phi^n, \quad a = \frac{1}{1 + \Delta t/T} \quad (2)$$

where n denotes the timestep number. Note that although the flow cases in the present work include homogeneous direction(s), no space averaging is made in Eq. 2.

In the LES region, the RANS velocities are prescribed as $v_i^{RANS} = \langle v_i^{LES} \rangle_T$, i.e.

$$S_i^{RANS} = \frac{\langle v_i^{LES} \rangle_T - \bar{v}_i^{RANS}}{\varepsilon} \quad (3)$$

where $\varepsilon = 10^{-10}$. The pressure is simply set as $\bar{p}^{RANS} = \langle p_i^{LES} \rangle_T$ and setting the pressure correction to zero. This means that, in reality, the RANS momentum equations are solved only in the S-RANS region. In the LES region they are merely transporting the turbulence quantities, k and ω , to ensure that correct values of k and ω are transported into the RANS region through the LES-RANS interface at $y = \delta_{S-RANS}$, see Fig. 1. The pressure, $\langle \bar{p}^{LES} \rangle_T$, at the LES-RANS interface is used as a boundary condition for the RANS equations in the S-RANS region.

2.1. The $k - \omega$ model

The Wilcox $k - \omega$ turbulence model reads

$$\begin{aligned} \frac{\partial k}{\partial t} + \frac{\partial \bar{v}_i k}{\partial x_i} &= P^k - \frac{k^{3/2}}{\ell_t} + \frac{\partial}{\partial x_j} \left[\left(\bar{v} + \frac{v_t}{\sigma_k} \right) \frac{\partial k}{\partial x_j} \right] \\ \frac{\partial \omega}{\partial t} + \frac{\partial \bar{v}_i \omega}{\partial x_i} &= C_{\omega 1} \frac{\omega}{k} P^k - C_{\omega 2} \omega^2 + \frac{\partial}{\partial x_j} \left[\left(\bar{v} + \frac{v_t}{\sigma_\omega} \right) \frac{\partial \omega}{\partial x_j} \right] \end{aligned} \quad (4)$$

2.2. The $k - \omega$ model in the DES solver

The DES equations are solved in the entire region, but they govern the flow only in the LES region, see Fig. 1. In the RANS regions, the lengthscale in Eq. 4 is computed as $\ell_t = k^{1/2}/(C_\mu \omega)$ and in the LES region it is taken from the IDDES model [6], i.e.

$$\ell_t = C_{LES} \Delta_{dw}, \quad \Delta_{max} = \max\{\Delta x, \Delta y, \Delta z\}, \quad \Delta_{dw} = \min(\max[C_{dw} d_w, C_w \Delta_{max}, \Delta_{nstep}], \Delta_{max}) \quad (5)$$

2.3. The $k - \omega$ EARSM model in the RANS solver

The steady RANS equations are solved in the entire region, but they govern the flow only in the RANS region, see Fig. 1. The Reynolds stresses, $\overline{v_i v_j}$, are computed from the two-dimensional explicit algebraic Reynolds stress model (EARSM) [5].



Figure 1: Grey color indicates the solver that drives the flow

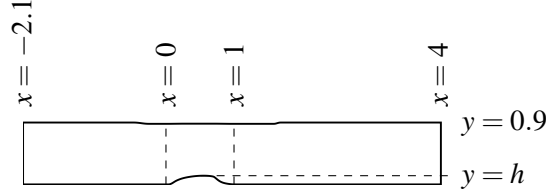


Figure 2: The domain of the hump. $z_{max} = 0.2$.

2.4. Initialization

The simulations are initialized as follows: first the 2D RANS equations are solved. Anisotropic synthetic fluctuations, $(\mathcal{V}'_i)_m$, are then superimposed to the 2D RANS field which gives the initial LES velocity field. The initial $\langle v_i^{LES} \rangle_T$ is also set from the 2D RANS field.

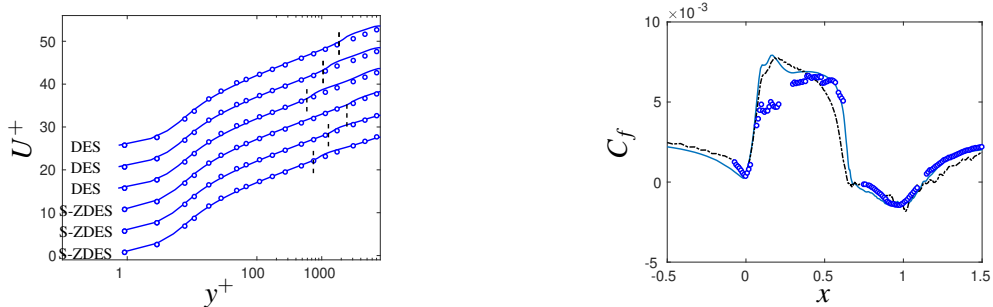
In order to compute $(\mathcal{V}'_i)_m$, synthetic fluctuations, $v'_{i,synt}$, are computed plane-by-plane ($y-z$) in the same way as prescribing inlet boundary conditions. The synthetic fluctuations in the $y-z$ planes are coupled with an asymmetric space filter

$$(\mathcal{V}'_i)_m = a(\mathcal{V}'_i)_{m-1} + b(v'_{i,synt,i})_m \quad (6)$$

where m denotes the index of the x_1 location and $a = \exp(-\Delta x_1/L_{int})$ and Δx_1 and L_{int} denote the grid size and the integral length scale, respectively ($L_{int} = 0.2$).

3. Results

The first test case is fully developed channel flow with periodic boundary conditions in streamwise (x) and spanwise (z) directions. The Reynolds number, $Re_\tau = u_\tau \delta / \nu$, is 8000 where δ denotes half-channel width. The size of the domain is $x_{max} = 3.2$, $y_{max} = 2$ and $z_{max} = 1.6$. The mesh has $32 \times 96 \times 32$ (x, y, z) cells. Figure 3a shows the velocity profiles for S-ZDES for three locations of δ_{S-RANS} and pure DES simulations for three locations of LES-RANS interface, $\delta_{S-RANS}^+ = 640, 1120$ and 2000 . The



(a) Velocity. $T = 100\delta/U_b$. Vertical black dashed lines: location of interface; \circ : Reichardt's law.

(b) Skinfriction. $T = 50h/U_{in}$. —: S-ZDES; - - - : DES

Figure 3: Channel and hump flow.

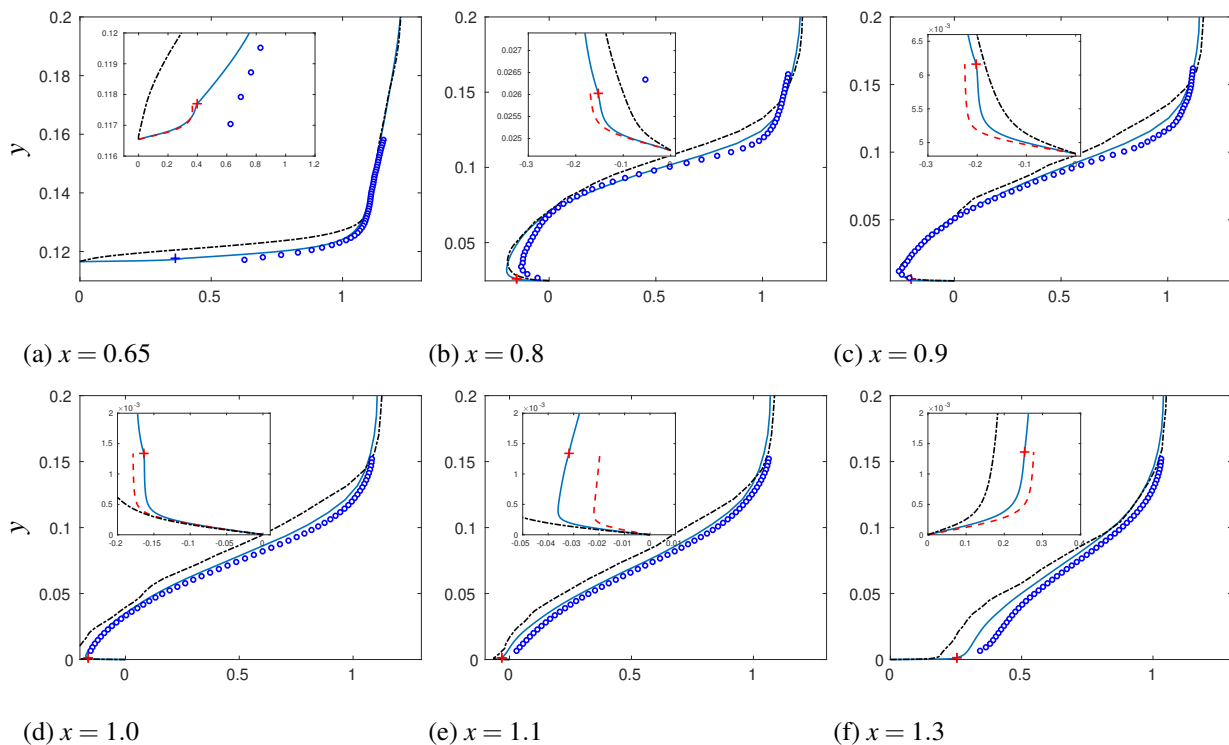


Figure 4: Hump flow: time-averaged velocities. — : DES solver; - - : RANS solver; ··· : DES; ○ : exp [7, 8]; + : LES-RANS interface.

three S-ZDES give no log-law mismatch whereas the three pure DES give a small log-law mismatch. Furthermore, it is seen that the location of the LES-RANS interface has a negligible impact.

The second test case is the flow over a two-dimensional hump, see Fig. 2. The Reynolds number of the hump flow is $Re_c = 936000$. The mesh has $386 \times 120 \times 32$ cells (x, y, z) and it is taken from the NASA workshop.¹ The inlet is located at $x = -2.1$ and the outlet at $x = 4.0$, see Fig. 2.

The inlet profiles are taken from a separate 2D RANS simulation with the same momentum thickness as the experimental velocity profiles. Anisotropic synthetic fluctuations are superimposed to the inlet velocity profile. Periodic boundary conditions are used in the spanwise direction (z). The interface between the S-RANS domain and the LES domain is defined along a gridline. Some results are presented in Figs. 3b and 4. As can be seen, the agreement with experiments is much better for S-ZDES than for pure DES. The inset in Fig. 4a reveals that the velocity profile is less full than the experimental one which probably is the reason why the predicted backflow is too strong at $x = 0.8$. The strong backflow at $x = 0.8$ is probably the reason to the slow recovery seen in Fig. 4f.

Consider the insets in Fig. 4. The DES solver and the RANS solver do not give exactly the same velocity profiles in the recirculation and the recovery regions. The reason is the limited time integration in Eq. 2. Here, $T = 50$ is used which should be compared to the averaging time ($T_{aver} = 260$ after an initial $T_{init} = 86$). The influence of T is weak but it exists and it will be discussed in the presentation.

References

- [1] H. Xiao, P. Jenna. *Journal of Computational Physics*, 231:1848–1865, 2012.
- [2] H. Xiao, Y. Sakai, R. Henniger, M. Wild, P. Jenna. *Computers & Fluids*, 88:653–662, 2013.
- [3] R. Tunstall, D. Laurence, R. Prosser, A. Skillen. *Computers & Fluids*, 157:73–83, 2017.
- [4] M. Breuer, S. Schmidt. *PAMM – Proc. Appl. Math. Mech.*, 14:647–650, 2014.
- [5] S. Wallin, A. V. Johansson. *Journal of Fluid Mechanics*, 403:89–132, 2000.
- [6] M. L. Shur, P. R. Spalart, M. Kh. Strelets, A. K. Travin. *Int. J. of Heat and Fluid Flow*, 29:1638–1649, 2008.
- [7] D. Greenblatt, K. B. Paschal, C.-S. Yao, J. Harris, N. W. Schaeffler, A. E. Washburn. AIAA-2004-2220, 2004.
- [8] D. Greenblatt, K. B. Paschal, C.-S. Yao, J. Harris. AIAA-2005-0485, 2005.

¹https://turbmodels.larc.nasa.gov/nasahump_val.html